Proceedings of the
Annual Stability Conference
Structural Stability Research Council
Atlanta, Georgia, April 21-24, 2026

Stability design of eccentrically loaded single angle struts - codes and practice

Mohammad Adil Dar[1], K. S. Vivek[2], N. Subramanian[3]

Abstract

Steel angles are commonly connected to other structural elements of the building system using gusset plates, resulting in connection through one leg only. This configuration introduces complexities in the structural behaviour arising from load eccentricity, end connection type, and the degree of rotational fixity. Various national design codes adopt distinct simplified approaches to address these complexities, leading to considerable variation in design strengths and safety margins. However, no detailed study has yet systematically examined these variations. This study reviews the design provisions of three widely adopted codes of practice viz. American (ANSI/AISC 360:2022), Indian (IS 800:2007 and its recent Draft Revision, IS 800:2025), and European (EN 1993-1-1:2005), which incorporate the simplified '*equivalent slenderness*' approach to *single angles connected at the ends by two or more bolts*. The design strengths of various equal-leg single angle sections were quantified in accordance with the three international design codes, with variations in slenderness ratios and yield strengths taken into account, and the outcomes were systematically compared. The results indicate significant discrepancies in design strength predictions across these codes, highlighting potential safety implications. While comparing the predicted strengths against the test strengths from a limited dataset available in the literature, the average ratios of test to predicted strengths, determined according to AISC 360 and IS 800 were 1.03 and 0.96, respectively, indicating a close correspondence between experimental and predicted values. In contrast, the same ratios based on EN 1993-1-1:2005 and IS 800 Draft 2025 were 0.76 and 0.80, respectively, revealing a noticeable deviation between the test and predicted strengths. Based on these findings, it is recommended that eccentrically loaded single angles (with two bolts in the end connection) be designed in accordance with the provisions of either AISC 360:2022 or IS 800:2007 to ensure adequate safety.

1. Introduction

Single angle sections are extensively used in roof trusses, transmission line towers, buildings, and bridges as primary load-carrying members or secondary members in the form of bracings (Figure 1). Their popularity stems from their simple profile, efficient use of cross-sectional area, ease of manufacturing and erection, and cost-effectiveness, despite their inherent asymmetry. Such members may often experience compression under various loading conditions. Typically, single angles are connected at the ends through bolting or welding to gusset plates or directly to a connecting member through one leg (Figure 2). This configuration introduces eccentric compression, as the compressive force does not act through the section's centroid, leading to complex instability (Subramanian, 2016). Further, the equal leg angles exhibit symmetry about the minor-principal (*v*-*v*) axis alone (Figure 2) and hence are singly

[1] Assistant Professor, BITS Pilani – Hyderabad Campus, India, <dar.adil@hyderabad.bits-pilani.ac.in>
[2] Assistant Professor, VVITU, Andhra Pradesh, India, <saivivek@vvit.net>
[3] Consulting Engineer, Maryland, USA, <drnsmani@gmail.com>

symmetric. In contrast unequal leg angles lack any type of symmetry, which introduces additional complexity to the buckling phenomenon.

Under compression, single angles may fail by flexural buckling (FB), torsional buckling (TB), or flexural-torsional buckling (FTB). Based on the experimental investigations conducted by Woolcock and Kitipornchai (1987) at Washington University between 1969 and 1972, angle struts in truss systems predominantly exhibit out-of-plane buckling. In particular, the buckling occurs in the direction perpendicular to the plane of the connected leg of the angle (i.e. buckling about axis *Y-Y* in Figure 2).

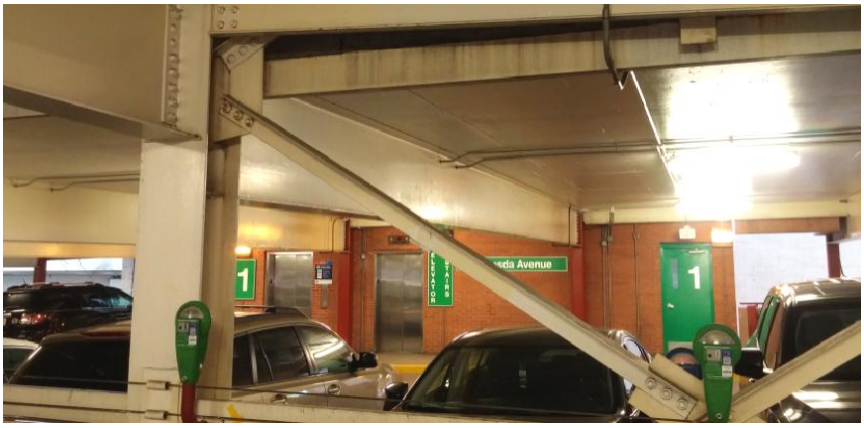

(a) Application in a braced frame of a building

(b) Application as bracing in bridge-deck

(c) Angle braces connected by two bolts

Figure 1. Application of bolted angle sections in practice

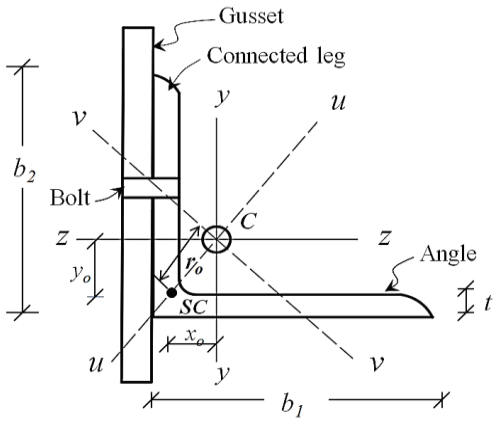

Figure 2. Single angle connected through one leg

An analytical second-order solution accounting for the in-plane and out-of-plane rotational restraint offered at end connections, inelasticity and bi-axial bending induced due to the eccentricity of load (i.e. *beam-column* behaviour) was proposed by Usami and Galambos (1971). Though the method could provide reliable solution, the procedure is tedious and requires computational effort which is not suitable for regular practice in design offices. Woolcock and Kitipornchai (1987) proposed a simplified design methodology for single angle struts provided as web members in planar trusses based on the research work carried out at Washington University. The method requires determining the out-of-plane bending moments based on the eccentricity at end connection. It is to be noted that the proposed method also follows the '*beam-column*' approach. According to the experimental investigation by Bathon et al (1993), eccentricity at the end connection significantly influenced the buckling load. Elgaaly et al (1992) reported that the bolted single angles can fail by global flexural / flexural-torsional buckling or combined local and flexural-torsional buckling. Angles with high global slenderness (i.e. ratio of effective length to the least radius of gyration) were prone to flexural buckling. Local buckling was noted in angles with legs of higher width-to-thickness ratio. The stress concentration at bolt holes was found to be high in case of single bolted angles due to which a lower capacity was exhibited in comparison to double bolted angles. Also, the axial capacity may not necessarily increase with decrease in global slenderness. The average ratio of failure load to the yield load capacity for the case of double bolted angles was found to be 28% greater than the single bolted angles.

The tests by Elgaaly et al (1992) and Bathon and Mueller (1993) also revealed that single angles behave differently in two-dimensional (planar) and three-dimensional (space) trusses. It is worth mentioning here that a set of modified equations were stated in ASCE / SEI 10-15 (2015) for determination of effective length of angles part of transmission towers (space trusses). Li et al (2023) investigated the behaviour of cross-bracing in transmission towers. It was stated that ASCE / SEI 10-15 (2015) and EN 1993-1-1: 2005 codes do not account the variation in axial force ratio on the buckling resistance. Equal leg angles were found to fail by out-of-plane buckling and the peak reduction in buckling resistance was found to be 40%. Design studies or tables for determining the axial capacity of eccentrically loaded angles based on the '*beam-column'* approach were also available (Walker (1991) and Sakla (2005)). Lutz (2006) evaluated the applicability of. '*equivalent slenderness'* – a simplified approach in determining the capacity of the single angles loaded eccentrically. The approach was found to be easy in comparison to the '*beam-column*' approach and resulted in a reasonably conservative estimate of the axial capacity.

In the past two decades, limited studies have contributed to understanding the behaviour of eccentrically loaded single angles. Bhilawe (2017) carried out experimental investigation on both single and double bolted angles with hinged boundary condition alone. The mean ratio of experimental to finite element strengths was about 0.90 for both single and double bolted specimens. In comparison to the single bolted specimens, axial capacity of double bolted specimens was greater by an average of 8.74% (with a minimum of 3.14% and maximum of 20.69% variation). Experimental tests on single angles with varying end support conditions were reported by Kettler et al (2019). The capacities of angles with knife-edge and hinged supports were nearly the same for either single or double bolted cases. The obtained load capacities were also comparable with the theoretical strengths predicted by the simplified '*equivalent slenderness*' approach based design procedure adopted in AISC 360-16. Double bolted angles with clamped supports exhibited higher capacities compared to those with hinged supports, a trend not observed in the single-bolted specimens. New design models which account for the joint stiffness were also proposed for both welded and bolted single angles

(Kettler et al (2021) and Kettler et al (2022)). Sofia et al (2023) and Gomes et al (2024) compared the numerical capacities with the provisions of European and American codes. Significant deviation was observed for the considered cases. The thickness of the gusset plate, boundary condition and material properties were found to influence the capacity of eccentrically loaded angles. Hussain et al. (2018), and Farhoud et al. (2024) compared results with the interaction equations (beam-column design approach) specified in the American and European codes of practice, although the existing simplified column design provisions were not examined.

Bashar and Amanat (2021) performed numerical validation of the three-dimensional truss adopted for experimental investigation by Elgaaly et al (1992), though a single two-dimensional truss was modeled by taking advantage of symmetry. For the case of double bolted angles, the provisions of ASCE code for transmission towers (ASCE / SEI 10-15) was found to predict the capacity (of target single angles) with an accuracy of 97%, whereas an accuracy of 88% was observed for IS 800 (IS 800:2007), though it was not clearly mentioned whether '*fixed*' or '*hinged*' classification of angle – to - gusset connection was considered. AISC 360-16 (ANSI / AISC, 2016) and other codes resulted in highly conservative (accuracy ranging from 66% to 69%) estimate of axial capacity. However, it must be noted that for the case of three-dimensional trusses i.e. transmission structures, different set of provisions available for determining the effective length in IS 802-1-2: 2016 code need to be adopted. Also the recent IS 800 2025 Draft introduces modified design provisions (the same was previously incorporated in the Amendment 2 to IS 800, released in 2024) that merits re-evaluation. A recent study by Vivek et al. (2024) highlighted significant disparities in design strengths predicted by IS 800:2007 and IS 800A2:2024 for the same sections. For the case of two-bolted and 'hinged' idealization of angle – to – gusset connection, a maximum increase in design capacity of about 104.84 % was observed by adopting provisions of IS 800A2:2024 in comparison to the earlier provisions of IS 800:2007. In general, except for few case of angles with low overall slenderness, provisions of IS800A2:2024 result in much higher capacities.

Based on the literature discussed above, it is evident that apart from the experimental research reported during 19th century, scarce experimental (or numerical) data exist on eccentrically loaded single angles. A major challenge lies in the lack of uniformity among different international design codes, in determining the capacity of eccentrically loaded single angle compression members. This results in significant variations in predicted design strengths for the same angle section with identical geometric and material properties. To the best knowledge of the authors, a study that provides a detailed comparison of the design strengths individual angles or angles within a two-dimensional truss system, as determined by various codes of practice, is not available. Hence, the present study aims to compare the design strengths of eccentrically loaded non-slender Indian steel angles (IS 808:2021) calculated using the provisions of IS 800:2007, IS 800 Draft 2025 (or IS 800A2:2024), American AISC 360:2022 (ANSI / AISC, 2022), and European EN 1993-1-1:2005 (EN, 2005) codes of practice. The scope of this study is confined to single equal-leg angle struts connected at ends by two or more bolts or equivalent welding, typically encountered in planar (two-dimensional) trusses, such as roof trusses.

2. American steel code (ANSI / AISC 360:2022) provisions

Section E5 of ANSI / AISC 360:2022 provides specifications for the design of single angle compression members. The least of the FB, TB and / FTB buckling capacities should be considered as the nominal capacity P_n. However, for sections with $b / t \leq 0.71 \sqrt{E/F_y}$ (where

b = width of leg, t = thickness of angle, E = modulus of elasticity and f_y = yield stress), FTB capacity may not be considered.

2.1. Flexural buckling (FB)

ANSI / AISC 360:2022 adopts a simplified '*effective slenderness*' approach to determine the flexural buckling strength of single angles while quantifying their design strength. In this method, the angle is assumed to be hinged at both ends, and the effects of loading eccentricity are incorporated by modifying the slenderness ratio L_c / r used in the design calculations (Lutz, 2006). This approach is specifically applicable to angle sections that are:

- Loaded through only one leg,
- Connected at the ends with a minimum of two bolts or an equivalent weld,
- Not subjected to transverse loading, and
- Have a slenderness ratio L_c / $r \leq 200$.

The modified slenderness ratio L_c/r is calculated using the following equations:

$$For\ \frac{L}{r_a} \leq 80$$

$$\frac{L_c}{r} = 72 + 0.75\,\frac{L}{r_a} \quad (1)$$

$$For\ \frac{L}{r_a} > 80$$

$$\frac{L_c}{r} = 32 + 1.25\,\frac{L}{r_a} \quad (2)$$

Where

L_c = Effective length of the member for buckling about the minor-axis
L = Length of the member measured between the work points located at the centerlines of the truss chords
r_a = radius of gyration about the geometric axis parallel to the connected leg, designated as axis '*a-a*'
r = radius of gyration (taken about minor-principal axis *v-v*)

Once $\frac{L_c}{r}$ is obtained, the flexural buckling capacity of the non-slender sections can be determined based on the procedure outlined in the Section E.3 of the code, as follows

$$P_n = F_n\,A_g \quad (3)$$

$$For\ \frac{L_c}{r} \leq 4.71\,\sqrt{\frac{E}{F_y}}$$

$$F_n = (0.658^{\frac{F_y}{F_e}})\,F_y$$

$$For\ \frac{L_c}{r} > 4.71\,\sqrt{\frac{E}{F_y}}$$

$$F_n = 0.877\,F_e \quad (4)$$

$$P_d = \phi_c\,P_n \quad (5)$$

Where

A_g = *Gross area of cross-section*
E = *Modulus of elasticity*
F_e = Elastic buckling stress
P_d = Design compressive strength (as per LRFD)

ANSI / AISC 360:2022 specifies the resistance factor 'ϕ_c' as 0.90 (as applicable for LRFD). For cases where a single bolt is used at each end, the eccentricity of loading must be explicitly

considered, and the member is required to be designed as a '*beam-column*' in accordance with Section H2 (as stated in the Commentary to Section E5). The simplified design approach based on '*effective slenderness*', outlined in the code (Commentary to Section E5), is derived from the work reported by Lutz (2006). This approach strategically assumes that the gusset or connecting member, referred to as the '*restraining member*' provides greater rotational restraint against buckling about the geometrical axis perpendicular to the plane of the end gusset (or the connected leg of the angle). Consequently, buckling about the geometrical axis parallel to the plane of the end gusset is more likely to govern the design.

2.2. Torsional buckling (TB) and Flexural-torsional buckling (FTB)

The elastic torsional or flexural-torsional buckling stress 'F_e' of equal leg single angles (singly-symmetric) can be determined using the following expression (Section E4 of AISC 360:2022)

$$F_e = \left(\frac{F_{eu}+F_{ez}}{2H}\right)\left[1 - \sqrt{1 - \left[\frac{4\,F_{eu}F_{ez}H}{(F_{eu}+F_{ez})^2}\right]}\right] \quad (6)$$

Where

F_{eu} = Critical stress about major principal axis 'u'

F_{ez} = Critical buckling stress about longitudinal axis 'z'

H = $1 - \frac{x_o^2+y_0^2}{r_o^2}$

G = Shear modulus

v = Poisson's ratio = 0.3

J = Torsional constant

C_w = Warping constant

$r_o^2 = \sqrt{x_0^2 + y_0^2}$

x_o, y_o = Co-ordinates of shear centre '*SC*' with respect to centroid '*C*'

L_{cz} = Effective length of the member with respect to 'z' axis

L_{cu} = Effective length of the member with respect to major principal axis 'u'

3. Indian steel code (IS 800:2007) provisions

Clause 7.5.1.2 specifies that the equivalent slenderness ratio (λ_e) must be accounted for when quantifying the flexural-torsional buckling (FTB) strength of a single angle subjected to eccentric loading through one leg. The design approach outlined in this clause is derived from the research conducted by Sambasiva Rao et al. (2003)

$$\lambda_e = \sqrt{k_1 + k_2\lambda_{vv}^2 + k_3\lambda_{\varphi}^2} \quad (7)$$

$$\lambda_{vv} = \frac{\left(\frac{l}{r_{vv}}\right)}{\varepsilon\sqrt{\frac{\pi^2 E}{250}}} \quad (8)$$

$$\lambda_{\varphi} = \frac{\left(\frac{b_1+b_2}{2t}\right)}{\varepsilon\sqrt{\frac{\pi^2 E}{250}}} \quad (9)$$

$$\phi = 0.5\,[1 + \alpha\,(\lambda_e - 0.2) + \lambda_e^2\,] \quad (10)$$

$$\chi = \frac{1}{\phi + \sqrt{\phi^2 - \lambda_e^2}} \quad (11)$$

$$f_{cd} = \frac{\chi f_y}{\gamma_{m0}} \quad (12)$$

$$P_d = A_e * f_{cd} \quad (13)$$

Where

χ = Stress reduction factor,
f_{cd} = Design compressive stress, Design compressive strength, P_d
l = centre – centre length of the supporting member
r_{vv} = radius of gyration about minor-principal axis '*v-v'*
λ_{vv} = non-dimensional slenderness accounting for minor-axis (*v-v*) flexural buckling
λ_{φ} = non-dimensional slenderness accounting for torsional buckling
b_1, b_2 = width of connected and outstanding legs respectively
k_1, k_2 and k_3 = constants accounting for end connection fixity, as presented in Table 1
t = thickness of leg of angle section
ε = yield stress ratio = $\sqrt{\frac{250}{f_y}}$; f_y = yield stress; γ_{m0} = 1.10
E = modulus of elasticity
α = Imperfection factor
= 0.49 for angle sections (corresponding to buckling class '*c*' as per Clauses 7.1.1 and 7.1.2.1)
A_e = Effective area = Gross cross-sectional area for non-slender sections

Table 1. Constants k_1, k_2 and k_3 as per IS 800:2007

No. of bolts at each end connection	Gusset / Connecting member fixity	k_1	k_2	k_3
≥ 2	Fixed	0.20	0.35	20
	Hinged	0.70	0.60	5
1	Fixed	0.75	0.35	20
	Hinged	1.25	0.50	60

It is important to highlight that the terms '*Fixed*' and '*Hinged*' conditions, as presented in Table 1, refer specifically to the rotational fixity provided by the end gusset or connecting member connection (Sambasiva Rao *et al* 2003).

4. New 2025 draft to IS 800 (IS 800:2025) provisions

The following modified design provisions were proposed recently, to determine the design strength of eccentrically loaded single angles considering both FTB and bending (i.e., FB). According to these provisions, the angle sections were classified under buckling class '*b*', with an associated imperfection factor 'α' of 0.36. The design compressive stress (strength) can be determined as per the following equations

$$f_{cde} = K_f \chi_{aa} f_y / \gamma_{m0} \quad (14)$$

$$K_f = k_1 + k_2 \lambda_{aa} + k_3 \lambda_{\phi} \quad (15)$$

$$\lambda_{aa} = \frac{(\frac{l_{aa}}{r_{aa}})}{\varepsilon\sqrt{\frac{\pi^2 E}{250}}} \quad (16)$$

$$\phi = 0.5\,[1 + \alpha\,(\lambda_{aa} - 0.2) + \lambda_{aa}^2\,] \quad (17)$$

$$\chi_{aa} = \frac{1}{\phi + \sqrt{\phi^2 - \lambda_{aa}^2}} \quad (18)$$

Where

λ_ϕ = same as expressed in Equation (16)

l_{aa} = centre-to-centre length of lateral support preventing translation of member perpendicular to *a-a* axis

r_{aa} = radius of gyration of the angle member about the *a-a* axis

a – a axis = centroidal axis parallel to the gusset or restraining member i.e. either '*z-z' or' y-y'* axis depending on which leg is connected. (In Figure 1, *a – a* axis is '*y-y'* axis)

α = 0.34 (corresponding to buckling class '*b'*)

k_1, k_2 and k_3 = constants accounting for end connection fixity, as presented in Table 2

Table 2. Constants k_1, k_2 and k_3 as per IS 800:2025 Draft

End connection	Gusset / Connecting member fixity	k_1	k_2	k_3
Fully welded or connected with two or more bolts	Fixed	0.798	0.563	-2.072
	Hinged	0.401	0.420	-1.040
Single bolt	Fixed	0.418	0.547	-1.400
	Hinged	0.374	0.415	-2.072

5. European steel code (EN 1993-1-1:2005) provisions

For non-slender sections, Clause 6.3.1.1 (3) specifies the procedure for determining the buckling resistance under FB, outlined as follows:

$$N_{b,\,Rd} = \frac{\chi\, A\, f_y}{\gamma_{m1}} \tag{19}$$

$$\chi = \frac{1}{\phi + \sqrt{\phi^2 - \lambda^2}} \leq 1 \tag{20}$$

$$\phi = 0.5\,[1 + \alpha\,(\lambda - 0.2) + \lambda^2\,] \tag{21}$$

$$\lambda = \sqrt{\frac{A\, f_y}{N_{cr}}} \text{ (for non-slender sections)}$$

$$= \frac{L_{cr}}{i}\,\frac{1}{\lambda_1} \tag{22}$$

$$\lambda_1 = \pi \sqrt{\frac{E}{f_y}} \tag{23}$$

$$\varepsilon = \sqrt{\frac{235}{f_y}} \tag{24}$$

Where

α = imperfection factor (0.34 for angle sections considering buckling class '*b*')

N_{cr} = elastic critical force of the relevant buckling mode

i = radius of gyration about relevant axis (i.e. about minor principal axis '*v*' for angles)

γ_{m1} = 1.0

Clause BB.1.2.1(B) of Annex BB emphasizes that for single angles used as web members in trusses, the effective slenderness ratio (λ_{eff}) about relevant axis, which accounts for the restraint provided by the end connections, must be considered for design as detailed below:

$$\lambda_{eff,\,v} = 0.35 + 0.7\,\lambda_v \tag{25}$$

$$\lambda_{eff,\,y} = 0.5 + 0.7\,\lambda_y \tag{26}$$

$$\lambda_{eff,z} = 0.5 + 0.7\,\lambda_z \quad (27)$$

Where, λ is calculated as per Eq. (22) with respect to relevant axis of buckling

Clause 6.3.1.4 stresses the need to evaluate the potential for reduced design strength due to TB or FTB. However, the Designer's Guide (Gardner and Netherton, 2011) clarifies that this clause primarily applies to thin-walled sections, while FB predominantly governs the failure of hot-rolled thick sections. Additionally, it is a widely accepted practice to design angle struts in trusses based solely on FB when dealing with non-slender sections, which may still be classified as thin-walled (Lam et al., 2014).

6. Comparison of design specifications of various codes

Unlike IS 800:2007 and IS 800:2025 Draft, the codes AISC 360:2022 and EN 1993-1-1:2005 do not explicitly classify the rotational fixity of end connections (bolted or welded) or connecting members as either '*fixed*' or '*hinged*'. Instead, in both AISC 360:2022 and EN 1993-1-1:2005, the angle strut or compression member is idealized as being hinged at both ends. While similar idealizations are made, IS 800:2007 and IS 800:2025 Draft (or Amendment 2 to IS 800, released in 2024) explicitly incorporate the effect of rotational restraint by classifying the end connections as '*fixed*' or '*hinged*' (Table 3), utilizing constants k_1, k_2 and k_3 as presented in Tables 1 and 2, respectively.

The Indian codes (IS 800:2007 and IS 800:2025 Draft) adopt a simplified approach for modifying the overall slenderness of the angle to account for the effect of the end connection, using an '*equivalent / effective slenderness ratio*' which disregards the eccentricity of load, for both single and double bolted angles. However, both AISC 360:2022 and EN 1993-1-1:2005 codes adopt the simplified approach only in case of angles connected at ends by two / more bolts or by equivalent welds and mandate to design as a '*beam-column'* (accounting for eccentricity of load) in case of single bolted angles (Table 3).

Table 3. Comparison of specifications of various codes of practice

End connection	Connecting member fixity	Codes of practice			
		AISC 360	IS 800:2007	IS 800:2025 Draft	EN 1993-1-1
≥ 2 bolts / Welded	Fixed	-	Simplified approach	Simplified approach	-
	Hinged	Simplified approach			Simplified approach
1 bolt	Fixed	-			-
	Hinged	Beam-column			Beam-column

7. Comparative study : Design strengths

The selected Indian Steel Angle (ISA) sections, conforming to IS 808:2021, meet the leg width-to-thickness ratio (b / t) requirements specified by the considered codes (Table 4) to qualify as '*non-slender*' sections. As previously mentioned, both the American and European codes do not adopt the simplified approach for single angles connected at ends by single bolts; this study focuses exclusively on the design of single angles connected with two or more bolts at either end (Figure 1(c)) and assumed to be hinged to maintain consistency. The relevant geometric properties of the selected angle sections are summarized in Table 5.

Table 4. Width – to – thickness ratio criteria for '*non-slender*' sections

Code of practice	Width – to – thickness ratio
AISC 360:2022	$\frac{b_1}{t} = \frac{b_2}{t} \leq 0.45\sqrt{\frac{E}{f_y}}$
IS 800:2007	$\frac{b_1}{t} = \frac{b_2}{t} \leq 15.7\varepsilon$; $\frac{b_1+b_2}{t} \leq 25\varepsilon$
IS 800A2:2024	
EN 1993-1-1:2005	$\frac{b_1}{t} = \frac{b_2}{t} \leq 15\ \varepsilon$; $\frac{b_1+b_2}{2t} \leq 25\varepsilon$

Table 5. Geometric details of selected ISA (IS 808:2021)

Angle	A (mm^2)	b_1 (=b_2) (mm)	t (mm)	b / t (mm)	$r_y = r_z$ (mm)	r_u (mm)	r_v (mm)
40 × 40 × 6	450	40	6	6.7	13.6	17.1	8.8
55 × 55 × 8	825	55	8	6.9	16.5	20.8	10.7
75 × 75 × 10	1310	75	10	7.5	22.7	28.5	14.7
90 × 90 × 12	2030	90	12	7.5	27.2	34.2	17.6
130 × 130 × 16	3910	130	16	8.1	39.4	49.7	25.4

[+]A = Area of cross-section; t = thickness; r_u, r_v = radius of gyration about major principal axis '*u-u*' and minor principal axis '*v-v*' respectively; r_z, r_y = radius of gyration about geometric centroidal axis '*z-z*' and '*y-y*' respectively

The design strengths 'P_d' of the selected angle sections were evaluated based on the specifications of IS 800:2007, IS 800:2025 Draft, AISC 360:2022, and EN 1993-1-1:2005 codes of practice for steel with yield strengths (f_y) of 250 MPa, 350 MPa, and 450 MPa, and for varying lengths of 0.5 m, 1.0 m, and 1.5 m, as presented in Tables 6–8. Figures. 3–5 illustrate the plots of the strength ratio (P_d / P_y) against the slenderness ratio (L / r_v) for the angle sections corresponding to the specified yield strengths.

For steel grade 250 (f_y = 250 MPa), on normalizing the design strengths quantified using IS 800 against those obtained using AISC 360, the mean ratio ($P_{d,IS}$ / $P_{d,AISC}$) was found to be 0.97, indicating close agreement with unity. This was accompanied by relatively low scatter, as evident from a Std. Dev. of 0.07 and a COV of 0.08. In comparison, the mean ratio for EN 1993 ($P_{d,EN}$ / $P_{d,AISC}$ = 1.16) was slightly higher, though the scatter remained moderate, with a Std. Dev. of 0.11 and a COV of 0.10. In contrast, the mean ratio for IS 800: 2025 Draft (P_{d,IS_25} / $P_{d,AISC}$ = 0.94) exhibited a significantly larger scatter, with a Std. Dev. of 0.31 and a COV of 0.33. It is worth noting that the P_{d,IS_25} / $P_{d,AISC}$ ratio ranged from a minimum of 0.6 to a maximum of 1.79, indicating considerable variability. This observed variability can be attributed to the relationship between the L / r_v and the normalized design strengths. As shown in Figure 3, $P_{d,AISC}$ / P_y, $P_{d,IS}$ / P_y and $P_{d,EN}$ / P_y exhibited a nearly linear decreasing trend with increasing L / r_v , with only minor deviations in a few data points. In contrast, the trend for P_{d,IS_25} / P_y displayed a non-linear relationship with L / r_v, characterized by an initial rise followed by a subsequent decline. This non-linear behavior was consistent across other steel grades (350 MPa and 450 MPa), although the specific values of the ratios varied (Tables 7 & 8 and Figures. 4 & 5).

Interestingly, the design strengths predicted by IS 800:2007 were greater than those predicted as per IS 800:2025 Draft, for L / $r_v \leq$ 68 (approx.) for f_y = 250 and 350 MPa and L / $r_v \leq$ 64

(approx.) for f_y = 450 MPa. However, beyond the stated limits of L / r_v, IS 800:2025 Draft provisions lead to much higher design strengths. In totality, the provisions of IS 800:2025 Draft resulted in a peak increase of axial capacity by 59%, 69.44% and 78.65% corresponding to yield strength (f_y) of 250 MPa, 350 MPa and 450 MPa respectively. Similarly, a maximum decrease of 34.87%, 34.73% and 34.51% were obtained.

In conclusion, when compared to AISC 360, EN 1993 resulted in a mean capacity increase of 16%, 38% and 60% for f_y of 250 MPa, 350 MPa and 450 MPa respectively. Also, $P_{d,\,EN} >> P_{d\,AISC}$, $P_{d,\,IS}$ and $P_{d,\,IS\_25}$ for $L / r_v < 140$, in case of f_y = 250 MPa and $L / r_v < 110$ (approx.) for f_y = 350 and 450MPa. Similarly, use of IS 800 resulted in an increase by 13% and 31% for f_y of 350 MPa and 450 MPa respectively, though close agreement was observed for f_y = 250 MPa. The authors believe that a similar conclusion cannot be drawn for IS 800:2025 Draft owing to the non-linear variation of normalized strength and high standard deviation (Std Dev), as previously discussed. Though a relatively close match between AISC 360 and IS 800:2007 was observed for all grades of steel and slenderness range, it should be noted that for the considered sections $b / t \leq 0.71\sqrt{E/F_y}$ and hence FTB was not accounted as per AISC 360 (though FTB was considered in IS 800 provisions).

Table 6. Design strengths (f_y = 250 MPa)

Angle section	L / r_v	Design strength, P_d (kN)				$\frac{P_{d,IS}}{P_{d,AISC}}$	$\frac{P_{d,IS\_25}}{P_{d,AISC}}$	$\frac{P_{d,EN}}{P_{d,AISC}}$
		AISC 360	IS 800	IS 800_25	EN 1993			
40 × 40 × 6	64.10	57.54	54.04	47.74	63.35	0.94	0.83	1.10
	128.21	37.81	35.48	46.69	47.61	0.94	1.23	1.26
	192.31	19.78	22.27	35.41	29.47	1.13	1.79	1.49
55 × 55 × 8	46.73	115.36	107.17	82.51	124.34	0.93	0.72	1.08
	93.46	89.34	83.09	90.34	103.88	0.93	1.01	1.16
	140.19	60.60	59.52	81.93	80.09	0.98	1.35	1.32
75 × 75 × 10	34.01	209.41	190.75	131.46	223.72	0.91	0.63	1.07
	68.03	176.76	165.21	148.06	195.73	0.93	0.84	1.11
	102.04	144.95	133.66	152.05	171.88	0.92	1.05	1.19
90 × 90 × 12	28.41	309.21	278.81	184.14	329.71	0.90	0.60	1.07
	56.82	270.03	251.68	206.84	294.25	0.93	0.77	1.09
	85.23	231.12	215.04	218.85	263.97	0.93	0.95	1.14
130 × 130 × 16	19.69	585.59	544.98	354.95	625.12	0.93	0.61	1.07
	39.37	499.96	518.30	401.15	550.47	1.04	0.80	1.10
	59.06	415.94	478.06	417.76	486.86	1.15	1.00	1.17
					Mean	0.97	0.94	1.16
					Std Dev	0.07	0.31	0.11
					COV	0.08	0.33	0.10

[+] $P_{d,AISC} = P_{d,\,AISC360}$, $P_{d,IS} = P_{d,IS800:2007}$, $P_{d,IS\_25} = P_{IS800:2025\ Draft}$ and $P_{d,EN} = P_{d,\,EN1993}$

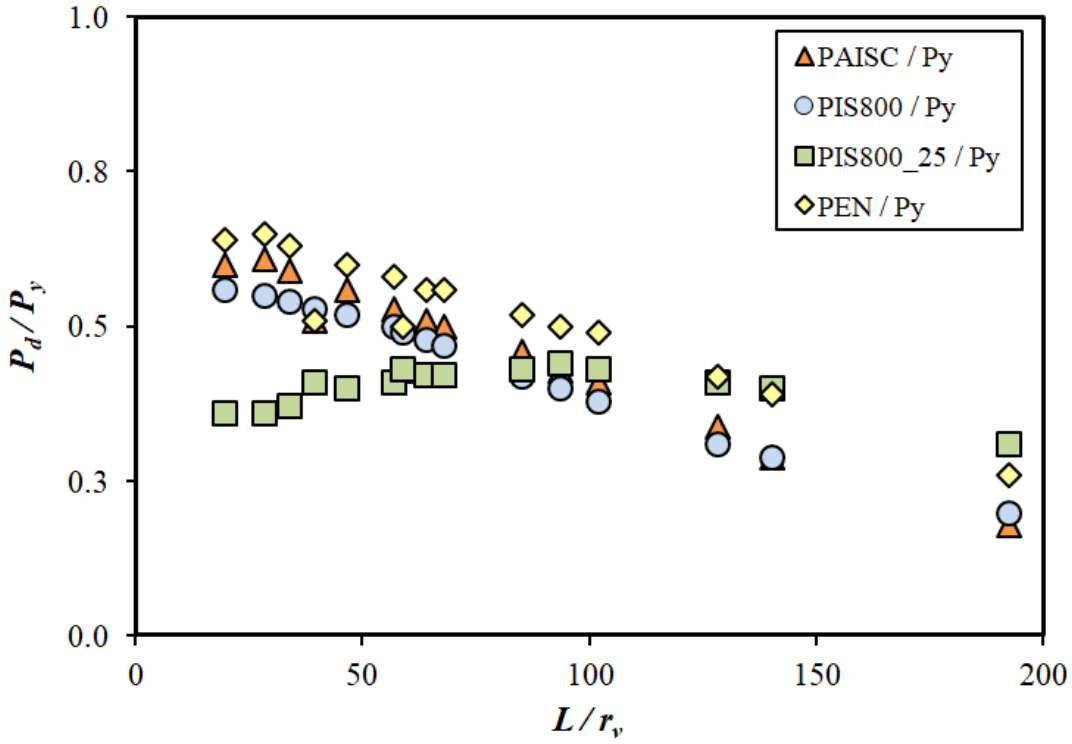

Figure 3. 'P_d / P_y' vs 'L / r_v' for f_y = 250 MPa

Table 7. Design strengths (f_y = 350 MPa)

Angle section	L / r_v	Design strength, P (kN)				$\frac{P_{d,IS}}{P_{d,AISC}}$	$\frac{P_{d,IS\_25}}{P_{d,AISC}}$	$\frac{P_{d,EN}}{P_{d,AISC}}$
		AISC 360	IS 800	IS 800_25	EN 1993			
40 × 40 × 6	64.10	64.26	70.51	66.63	84.79	1.10	1.04	1.32
	128.21	37.81	41.63	58.73	56.14	1.10	1.55	1.48
	192.31	19.78	24.54	41.58	32.03	1.24	2.10	1.62
55 × 55 × 8	46.73	133.52	143.72	115.36	168.33	1.08	0.86	1.26
	93.46	93.17	102.87	121.87	136.13	1.10	1.31	1.46
	140.19	60.60	68.77	100.98	92.41	1.13	1.67	1.52
75 × 75 × 10	34.01	248.3	259.72	182.27	305.38	1.05	0.73	1.23
	68.03	195.85	213.81	205.73	261.30	1.09	1.05	1.33
	102.04	148.67	162.99	201.62	219.83	1.10	1.36	1.48
90 × 90 × 12	28.41	370.35	381.82	254.21	451.72	1.03	0.69	1.22
	56.82	306.37	331.95	288.62	395.79	1.08	0.94	1.29
	85.23	246.12	269.92	298.82	348.15	1.10	1.21	1.41
130 × 130 × 16	19.69	696.65	750.62	489.91	854.31	1.08	0.70	1.23
	39.37	558.33	700.31	557.38	736.72	1.25	1.00	1.32
	59.06	431.09	627.51	559.09	636.55	1.46	1.30	1.48
					Mean	1.13	1.17	1.38
					Std Dev	0.11	0.38	0.12
					COV	0.09	0.33	0.09

[+] $P_{d,AISC} = P_{d,\ AISC360}$, $P_{d,IS} = P_{d,IS800:2007}$, $P_{d,IS\_25} = P_{IS800:2025\ Draft}$ *and* $P_{d,EN} = P_{d,\ EN1993}$

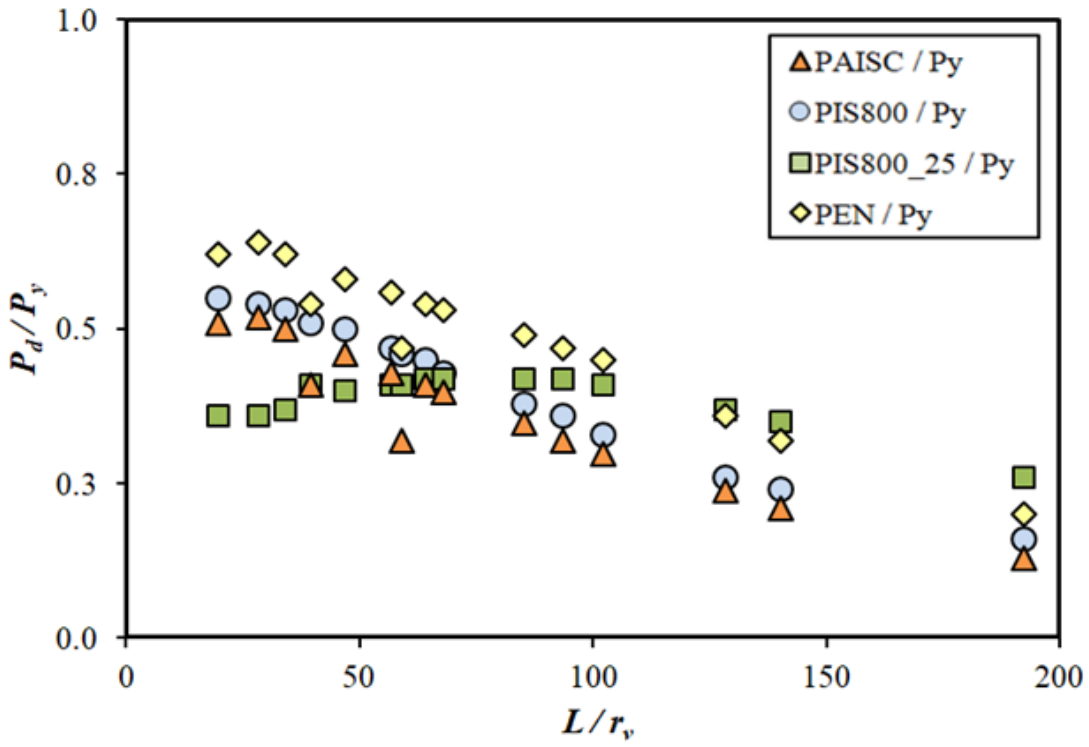

Figure 4. 'P_d / P_y' vs 'L / r_v' for f_y = 350 MPa

Table 8. Design strengths (f_y = 450 MPa)

Angle section	L / r_v	Design strength, P (kN)				$\frac{P_{d,IS}}{P_{d,AISC}}$	$\frac{P_{d,IS\_25}}{P_{d,AISC}}$	$\frac{P_{d,EN}}{P_{d,AISC}}$
		AISC 360	IS 800	IS 800_25	EN 1993			
40 × 40 × 6	64.10	65.77	84.77	84.84	104.86	1.29	1.29	1.59
	128.21	37.81	46.03	67.95	61.84	1.22	1.80	1.64
	192.31	19.78	26.04	46.52	33.65	1.32	2.35	1.70
55 × 55 × 8	46.73	141.93	177.2	147.8	210.32	1.25	1.04	1.48
	93.46	93.17	118.37	148.94	160.22	1.27	1.60	1.72
	140.19	60.60	75.24	115.48	100.38	1.24	1.91	1.66
75 × 75 × 10	34.01	270.37	324.89	232.24	384.27	1.20	0.86	1.42
	68.03	199.11	255.21	260.59	322.43	1.28	1.31	1.62
	102.04	148.67	185.35	242.43	252.38	1.25	1.63	1.70
90 × 90 × 12	28.41	407.36	480.33	322.82	570.22	1.18	0.79	1.40
	56.82	318.99	403.01	368.34	491.71	1.26	1.15	1.54
	85.23	246.12	314.01	370.10	424.42	1.28	1.50	1.72
130 × 130 × 16	19.69	761.12	949.56	621.90	1076.13	1.25	0.82	1.41
	39.37	571.44	869.90	707.06	911.14	1.52	1.24	1.59
	59.06	431.09	758.52	678.21	770.51	1.76	1.57	1.79
					Mean	1.31	1.39	1.60
					Std Dev	0.14	0.42	0.12
					COV	0.10	0.30	0.08

[+] $P_{d,AISC} = P_{d,\ AISC360}$, $P_{d,IS} = P_{d,IS800:2007}$, $P_{d,IS\_25} = P_{IS800:2025\ Draft}$ and $P_{d,EN} = P_{d,\ EN1993}$

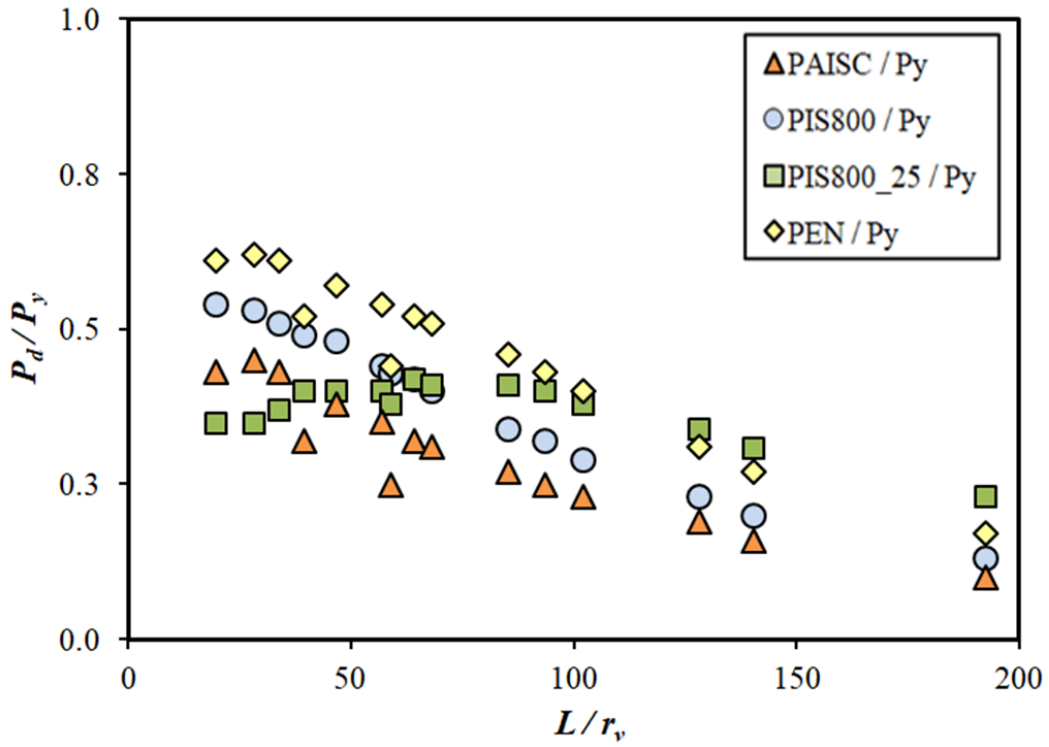

Figure 5. 'P_d / P_y' vs 'L / r_v' for f_y = 450 MPa

8. Comparative study : Experimental data

In the previous section, the design strengths of ISAs in accordance with provisions of the considered codes of practice were presented. This section focuses on comparing the nominal capacities based on the recently reported experimental test results. Though Elgaaly et al (1992) and Bathon and Mueller (1993) reported tests on eccentrically loaded single angle struts connected at their ends by two or more bolts, either the sections were found to be '*slender*' or adequate data required for design was not available and hence not considered in the present study. However, two recent studies viz. Bhilawe et al (2017) and Kettler et al (2019) were available, though very limited tests pertaining to the '*hinged end*' boundary condition were reported. The nominal strengths 'P_n', as per the considered codes of practice (i.e. P_{n_AISC}, P_{n_IS800}, $P_{n\_IS800\_25}$ and P_{n_EC3}), were determined by assuming partial safety factors to be unity, for comparison with the corresponding test strengths, as shown in Table 9.

Table 9. Test – to – nominal strength ratios

Specimen	L / r_{vv}	L / r_{aa}	P_{Test} / P_{n_AISC}	P_{Test} / P_{n_IS800}	$P_{Test} / P_{n\_IS800\_25}$	P_{Test} / P_{n_EC3}
Bhilawe (2017)						
S6A	62.17	39.53	1.06	0.99	1.11	0.90
S6B	114.56	72.83	1.01	0.96	0.73	0.78
S6C	156.25	99.34	1.25	1.11	0.72	0.91
Kettler et al (2019)						
B1	96.11	61.32	1.00	0.99	0.87	0.80
B2	148.10	94.65	0.95	0.88	0.61	0.72
B3	183.97	117.28	0.93	0.82	0.51	0.68
		Mean	1.03	0.96	0.76	0.80
		Std Dev	0.11	0.10	0.21	0.09
		COV	0.11	0.10	0.28	0.12

The mean of P_{Test} / P_{n_AISC} and P_{Test} / P_{n_IS800} ratios were obtained as 1.03 and 0.96 respectively, indicating a reasonably close agreement of the nominal strengths with the corresponding test strengths. However, the mean of $P_{Test} / P_{n\_IS800\_25}$ and P_{Test} / P_{n_EC3} ratios were 0.76 and 0.80 respectively, indicating significant disparity between the nominal and test strengths i.e. much higher capacity predicted as per the respective codes. Though more research data is required to arrive at a comprehensive and reliable conclusion, it is imperative that the design of eccentrically loaded single angle struts (of plane or two-dimensional trusses) be carried out in accordance with either AISC 360: 2024 or IS 800: 2007 in view of structural safety, based on the present investigation of the limited research data available.

10. Conclusions

This study presented a comparative evaluation of design strengths for eccentrically loaded single angle struts connected at ends by two bolts or of equivalent weld as per the simplified '*equivalent slenderness*' approach adopted by AISC 360:2022, EN 1993-1-1:2005, IS 800:2007 and IS 800: 2025 Draft. Also, for the available test results reported recently in the literature, the nominal strengths were determined as per the considered codes of practice and compared. The findings offer critical insights into the variations in design approaches across these standards and their implications for structural safety and adequacy. The key conclusions summarized are as follows:

- A significant variation was observed among the predicted design strengths determined as per AISC 360:2022, IS 800:2007, IS 800:2025 Draft and EN 1993-1-1:2005, particularly for f_y = 350 and 450 MPa.
- Among all the considered codes, EN 1993-1-1:2005 resulted in peak design strength compared to the other codes for $L / r_v <$ 140 (approx.) in case of f_y = 250 MPa and for $L / r_v <$ 110 (approx.) in case of f_y = 350 and 450 MPa. For L / r_v greater than the stated limits, IS 800:2025 Draft lead to peak design strengths.
- For f_y = 250 MPa, the design strengths obtained as per AISC 360:2022 and IS 800:2007 were found to be nearly the same (Mean P_{IS} / P_{AISC} = 0.97). However, for f_y = 350 MPa and 450 MPa, the mean P_{IS} / P_{AISC} was found to be 1.13 and 1.31 respectively indicating significant variation.
- The *mean* normalized design capacity $P_{d,EN} / P_{d,\ AISC}$ was found to be 1.16, 1.38 and 1.60 corresponding to f_y of 250, 350 and 450 MPa respectively. These were the highest in comparison to $P_{d,IS} / P_{d,AISC}$ and $P_{d,ISA2} / P_{d,\ AISC}$, clearly demonstrating that the provisions of EN 1993-1-1:2005 predict much higher capacity in comparison to AISC 360:2022, IS 800:2007and IS 800:2025 Draft.
- Though the obtained design strengths as per AISC 360:2022 and IS 800:2007 were close, it should be noted that the considered sections donot require FTB consideration as per AISC360, whereas IS800 provisions account for FTB.
- The modified provisions incorporated in IS 800:2025 Draft lead to significant variation in predicted design strength compared to other codes including IS 800:2007. The variation of design strength to yield capacity ratio with respect to the slenderness ratio (L / r_v) was found to be non-linear, unlike that of AISC 360-2022, IS 800:2007 and EN 1993-1-1:2005, for which a nearly linear trend was observed.
- Due to the non-linear variation of design strength with respect to slenderness ratio, standard deviation of $P_{d,ISA2} / P_{d,AISC}$ was obtained as 0.31, 0.38 and 0.41 corresponding to f_y of 250, 350 and 450 MPa.
- In comparison to IS 800:2007, the modified provisions brought out in IS 800:2025 Draft lead to peak increase of axial capacity by 59%, 69.44% and 78.65% corresponding to f_y of 250 MPa, 350 MPa and 450 MPa respectively. Similarly, a maximum decrease of 34.87%, 34.73% and 34.51% were noted.

- Based on the presented comparison with the available scarce experimental data, it was found that both AISC 360:2022 and IS 800:2007 provisions lead to reasonably accurate prediction of mean nominal capacity (P_{Test} / P_{n_AISC} = 1.03 and P_{Test} / P_{n_IS800} = 0.96). Mean $P_{Test} / P_{n\_IS\_25}$ and P_{Test} / P_{n_EN} were obtained as 0.76 and 0.80 indicating significant discrepancy.

In conclusion, significant variation in predicted nominal or design strengths across the considered codes raise safety concern for single angle struts. Based on the findings of the present study and the scarce research data available at present, the authors express that the designers may choose to design or cross-check as per the provisions of either AISC 360:2022 or IS 800:2007 in design of single angle struts (part of two-dimensional structural systems) for ensured safety.

References

ANSI / AISC. 2022. *Specification for structural steel buildings*. ANSI / AISC 360. Chicago: American Institute of Steel Construction.

ANSI / AISC. 2016. *Specification for structural steel buildings*. ANSI / AISC 360. Chicago: American Institute of Steel Construction.

ASCE / SEI. 2015. Design of latticed steel transmission structures. ASCE / SEI 10, Virginia: American Society of Civil Engineers.

Bashar, I., Amanat, K. M. 2021. "Comparison of codes for axial compression capacity of eccentrically loaded single angles." *J. Constr. Steel Res.* 185: 106829.

Bathon, L, and Mueller, W. 1993. "Ultimate load capacity of single steel angles," *J. Struct. Eng. ASCE.* 119: 279-300.

Bhilawe, J. 2017. "Study of equal angle subjected to compression for bolted end connection.", *J. Inst. Eng. India Ser. A.* 99: 123–132.

BIS (Bureau of Indian Standards). 2007. General constructions in steel – code of practice. IS 800. New Delhi, India: BIS

BIS (Bureau of Indian Standards). 2016. Use of structural steel in overhead transmission line towers: Design strengths. IS 802 – Part 1 – Sec 2. New Delhi, India: BIS

BIS (Bureau of Indian Standards). 2021. Hot rolled steel beam, column, channel and angle sections – dimensions and properties. IS 808. New Delhi, India: BIS

BIS (Bureau of Indian Standards). 2024. Amendment 2 to General constructions in steel – Code of practice. IS 800. New Delhi, India: BIS

BIS (Bureau of Indian Standards). 2025. Draft Indian Standard for General Construction in Steel – Code of Practice (Fourth Revision of IS 800), CED 07 (27869) WC. New Delhi, India: BIS

Elgaaly, M., Dagher, H., and Davids, W. 1992. "Behavior of single-angle-compression members," *J. Struct.Eng. ASCE.* 117: 3720-3741.

Farhoud, H., Bezas, M. Z., Demonceau, J. F., Jaspart, J. J., and Vayas, I. 2024. "Buckling strength of rolled angles: Comparison between International codes," *J. Struct. Eng. ASCE.* 150 (9): 04024122

Gardner, L., and Nethorcot, D. 2011. *Designer's Guide to Eurocode 3: Design of Steel Buildings*, 2nd Ed. Marshwall, London: ICE Publishing, Thomas Telford Limited.

Gomes Jr. J. O., Carvalho, H,, Simoes da Silva, L., Ferreira Filho, J. O., Lavall, A. 2023. "Assessment of design procedures for the buckling resistance of hot-rolled steel equal leg angles under concentric and eccentric compression." *Structures*. 57: 105308.

Hussain, A., Liu, Y. P., and Chan, S. L. 2018. "Finite element modeling and design of single angle member under bi-axial bending," *Structures*. 16: 373-389.

Kettler, M., Taras, A., Unterweger, H. 2017. "Member capacity of bolted steel angles in compression- Influence of realistic end supports." *J. Constr. Steel Res*. 130: 22‑35.

Kettler, M., Lichtl, G., Unterweger, H. 2019. "Experimental tests on bolted steel angles in compression with varying end supports." *J. Constr. Steel Res*. 155: 301‑315.

Kettler, M., Unterweger, H., Zaucher, P. 2022. "Design model for the compressive strength of angle members including weld end-joints." *Thin-Walled Struct.* 184: 106778.

Lam, D., Ang, T. C., and Chiew, S.P. 2016. *Structural Steel Work: Design to Limit State Theory*, Boca Raton, FL: CRC Press.

Li, Y., Yan, Z., Zhou, D., Ren, Q., Hua, C., Zhong, Y. 2023. "Analysis of the stability behavior of cross bracings in transmission towers based on experiments and numerical simulations." *Thin_Walled Struct.*

185: 110554.
Lutz, L. A. 2006. “Evaluating Single-Angle Compression Struts Using an Effective Slenderness Approach.” *Engineering Journal, AISC*. 43 (4): 241-246.
Sakla, Sherif S. S. 2001. “Tables for the design strength of eccentrically loaded single angle struts.” *Engineering Journal, AISC*. 38: 127-136.
Sakla, Sherif S. S. 2005. “Performance of the AISC LRFD specification in predicting the capacity of eccentrically loaded single-angle struts.” *Engineering Journal, AISC*. 42 (4) : 239-246.
Sambasiva Rao, S., Satish Kumar, S. R., Kalyanaraman, V. 2003. “Numerical study on eccentrically loaded hot rolled steel single angle struts.” In Proc., Civil – Comp Press, Edinburgh, UK, 2003. 10.4203/ccp.77.44
Sofia, A., Bezas, M. Z., Demonceau, J. F., Vayas, I., Maesschalck, J., Anwaar, M. O., and Jaspart, J. P. 2023. “Buckling resistance of angle bracing members with one-leg end connections.”, Ce/papers, 6 (3-4): 1157-1162.
Subramanian, N. 2016. *Design of steel structures-limit states method*, New Delhi, India: Oxford University Press.
Usami, T., Galambos, T. V. 1971. “Eccentrically loaded single angle columns.” *IABSE Publ.*, 31: 153-184.
Vivek, K. S., Dar, M.A., and Subramanian, N. 2024. “Efficacy of IS code provisions for design of eccentrically loaded single angle compression members.”, *Buildings*. 14 (9): 2990.
Walker, W. W. 1991. “Tables for Equal Single Angles in Compression.” *Engineering Journal, AISC*. 28: 65-68.
Woolcock, S. T., and Kitipornchai, S. 1987. “Design of single angle web struts in trusses.*” J. Struct. Eng, ASCE.* 112: 1327-1345.